RESOLVING INLAND WATERWAYS WITH CYGNSS

Christopher Ruf[1], Clara Chew[2], Cynthia Gerlein-Safdi[3], April Warnock[4]

1. University of Michigan, Ann Arbor, MI USA
2. University Corporation for Atmospheric Research, Boulder, CO USA
3. Lawrence Berkeley National Laboratory, Berkeley, CA USA
4. SRI International, Ann Arbor, MI USA

ABSTRACT

Observations made by the NASA Cyclone Global Navigation Satellite System (CYGNSS) of inland waterways can be used to resolve changes in water boundaries on time scales from days to weeks to months. An example of change on a daily time scale is the response of river width to rapid changes in stream flow rate. An example of change on a weekly time scale is the flood inundation caused by a land falling hurricane. And an example of change on a monthly time scale is the expansion and contraction of a major river delta due to seasonal monsoon rains. CYGNSS measurements of each of these phenomena are presented, and related considerations and implications of its measurement capability are discussed.

***Index Terms*—** CYGNSS, GNSS-R.

1. INTRODUCTION

The Cyclone Global Navigation Satellite System (CYGNSS) is a NASA mission with a flight segment consisting of 8 spacecraft in a common 35^o inclination circular orbit at 520 km altitude. Each spacecraft carries a 4-channel GPS receiver designed to measure L1 signals reflected from the Earth's surface [1-2]. The combination of 8 spacecraft, 4 receiving channels, and a low inclination orbit (to restrict latitudinal coverage) results in a mean revisit time of ~7 hours between 35S and 35N latitude [3]. CYGNSS was launched in December 2016 and has since demonstrated its ability to estimate ocean surface wind speed as a science data product from its engineering measurements of the quasi-specular forward scattering cross section of the ocean surface [4-6]. While originally intended and designed as an ocean winds mission, science operations and data collection are maintained with a 100% duty cycle for ease of operations. As a result, measurements over land are produced with a similarly high temporal sampling cadence. What was originally designed as a system to resolve short time scale tropical cyclone processes such as their rapid intensification phase might also be used to resolve short time scale processes over land such as flood inundation after a hurricane landfall or extreme inland precipitation event, changes in river delta size and shape due to seasonal monsoonal rains, and the overtopping of riverbanks due to sudden increases in stream flow.

Frequent temporal sampling is a necessary but not sufficient condition for CYGNSS to be able to resolve rapid changes in the spatial extent of inland waterways. Its measurements must also be able to discriminate between inland water and surrounding land surfaces, and they must be able to resolve the water bodies with sufficient spatial resolution to detect the changes of interest. Fortunately, both of these requirements have been found to be satisfied by almost all CYGNSS passes over inland waterways. One reason is the large difference between the dielectric constants of water and land surfaces, with water typically being much higher. This tends to increase the observed scattering cross section of the water surface above that of the land. More importantly, inland water surfaces are typically smooth enough to support predominantly coherent specular forward scattering, as opposed to

DOI: 10.1109/IGARSS47720.2021.9554192

.0 1 2 33,) 0) 1

the predominantly incoherent quasi-specular forward scattering that occurs over land. In terms of their impact on the measurements, the difference between these two scattering processes can be significant. Coherently scattered signals tend to be ~30 dB higher in signal strength [7-8], making them easy to differentiate from the much weaker signals scattered by the surrounding land surfaces. In addition, the fundamental spatial resolution associated with the two scattering processes is very different. The spatial resolution of incoherently scattered signals is largely determined by the temporal autocorrelation and bandwidth of the GPS pseudorandom noise modulation [9]. In practice, this corresponds to a spatial resolution of 10-20 km for CYGNSS, depending on the incidence angle of the observation [6]. With coherently scattered signals, the spatial resolution is largely determined by the first Fresnel zone of the surface reflection [7]. This corresponds to a spatial resolution of 300-800 m for CYGNSS, also depending on incidence angle [10].

These properties of CYGNSS measurements – continuous (100% duty cycle) operation, frequent (sub-daily) revisit time, clear discrimination between inland water and land, and better spatial resolution due to coherent scattering – combine to enable short time scale dynamics of inland waterways to be resolved. This capability has many potential uses, ranging from investigations of hydrologic processes to support for disaster management. Following are illustrative examples of measurements made by CYGNSS of a variety of different inland waterways, selected to highlight its capabilities and motivate their use for both science and applications.

2. "FIRST LIGHT" IMAGE OF INLAND WATERWAYS

The earliest reported example of CYGNSS measurements of inland waterways is the image shown in Fig. 1 of the Amazon River basin and associated tributaries. This image was created by Clara Chew and presented at the first CYGNSS science team meeting after launch, in May 2017. It is composed of measurements made over a one

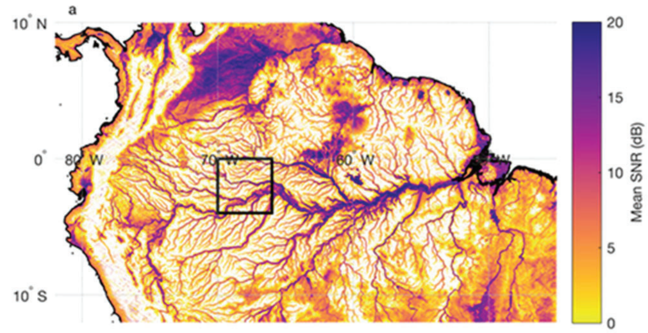

Figure 1. "First light" inland waterbody image by CYGNSS, of the Amazon River basin.

month period. To say that the other members of the science team were pleasantly surprised by the resolution and clarity of this image would be a gross understatement. The high spatial resolution in the figure is especially noticeable in the well resolved smaller tributaries. The concept of enhanced spatial resolution in the presence of coherent scattering was well known at the time. What was surprising and not so well appreciated was the fact that inland water bodies were sufficiently and consistently smooth that scattering from them would almost always be coherent.

The clarity of the image across such a large portion of the South American continent results from an important geolocation property of GNSS-R measurements. Whereas most visible, infrared and microwave imagers require knowledge of spacecraft attitude and pointing by the antenna or optics to geolocate their measurements, GNSS-R requires only knowledge of the location of the spacecraft to geolocate the point of specular reflection on the surface. Spacecraft attitude and antenna pointing are irrelevant. This allows measurements accumulated over multiple satellite overpasses of a region to be composited easily and accurately without the need for the often-painstaking geolocation corrections that would otherwise be required. This property is especially noteworthy in the case of a mission like CYGNSS, which uses low cost microsatellites that have less capable attitude control or knowledge than is typical with larger and more costly platforms. Note also that smaller tributaries in the Amazon region are often obscured by vegetation canopies. The long (19 cm) wavelength used by GPS is able to penetrate through the vegetation.

3. RESOLVING FLOOD INUNDATION

The rapid refresh rate of the CYGNSS constellations permits its measurements to be used to detect sudden changes in the extent of water bodies, such as result from flooding caused by a land falling hurricane. An example of this is given in Fig. 2, which shows maps of surface reflectivity before and after the passage of Hurricane Isaias in August 2020. The 'before' image is composed of measurements made during 10-25 July 2020 and the 'after' image during 28 July – 6 August 2020. In the insert in the figure, the change in reflectivity is shown across the Dominican Republic. The eastern portion of the island experienced extensive flooding in communities surrounding the capital city of Santo Domingo. These regions are highlighted in the image as areas with the largest change (increase) in reflectivity, which was caused by the flooding.

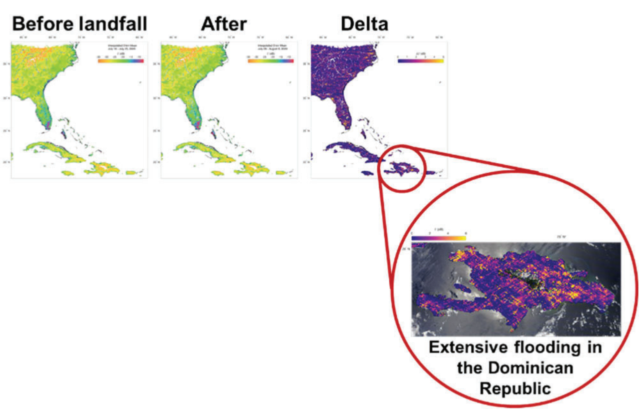

Figure 2. Images of surface reflectivity before (Jul 2020) and after (Aug 2020) Hurricane Isaias landfall. The inset shows the change in reflectivity for the Dominican Republic. The largest changes are associated with extensive flooding near the capital city of Santo Domingo.

4. RESOLVING SEASONAL VARIABILITY AND CREATING WATER MASKS

Major river deltas can experience seasonal variations in their water boundaries, in particular if they are in regions that experience significant monsoonal rainfall. An example of this is the Okavango Delta in Botswana. Fig. 3 shows water masks created from CYGNSS observations in December 2017 – Feb 2018 (left) and June – August 2018 (right). The large increase in water extent during the summer months is the result of runoff from heavy monsoon rains during the spring in upstream portions of the Okavango River that feeds into the delta. Generation of these water masks relies on a random walker segmentation of the CYGNSS reflectivity observations to account for gaps between the locations of the specular reflections [11]. Gaps in the spatial coverage of reflectivity maps are an important consideration for any application that requires continuous coverage.

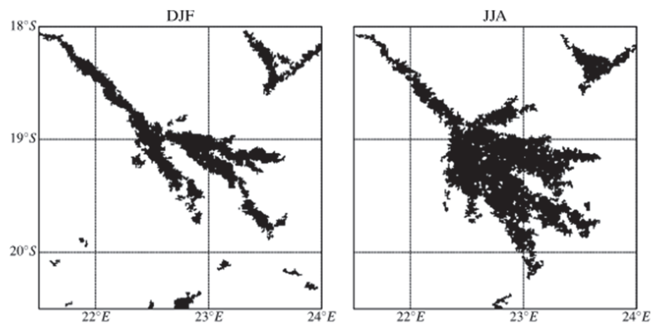

Figure 3. Watermasks of the Okavango Delta in Botswana. The delta is largely dry with rivers running through it during December-January-February (left panel) but expands in June-July-August (right panel) due to spring rainfall upstream [11].

5. RESOLVING RIVER WIDTH AND ESTIMATING STREAM FLOW

In addition to combining many overpasses of a region by the entire CYGNSS constellation to create 2-D images of water bodies, the specular point track from an individual satellite can be used to measure the 1-D cross section of a water body. This is illustrated in Fig. 4, which shows a series of 5 tracks crossing the Pascagoula River in Mississippi, USA over 7 days in April 2019 during a flood event caused by heavy precipitation [8]. A USGS stream gauge measurement at each overpass time recorded flow rates of between 800 and 1500 m^3s^{-1}. The reflectivity tracks show a narrow spike at each river crossing due to the stronger reflection from water. The width of the spike, referred to as the Associated GNSS-R Width (AGW) of the river, is an indication of its width at the time of the overpass. The AGW is shown in [8] to be highly correlated with the flow rate measured at the same time. This suggests that spaceborne GNSS-R measurements may be able to provide river stream flow information globally on a regular basis.

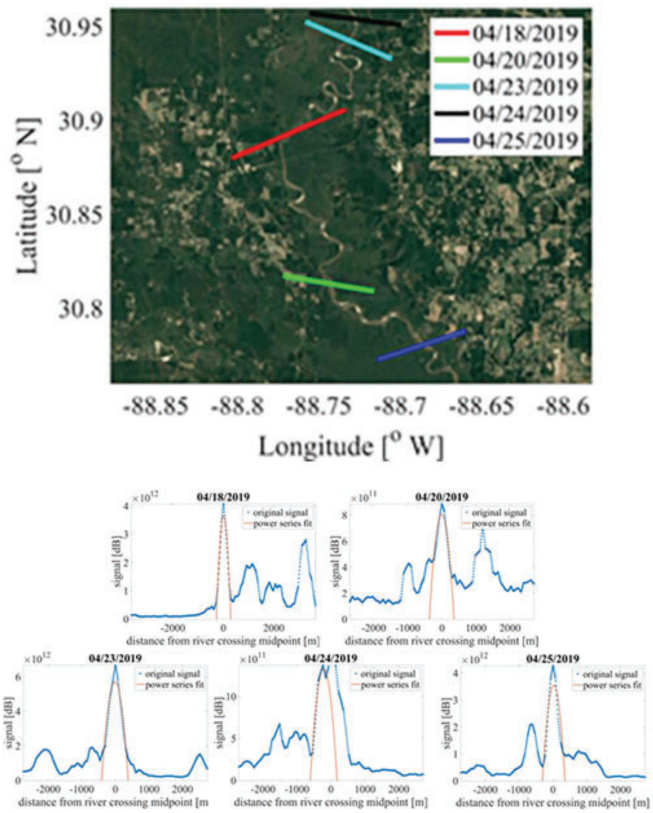

Figure 4. *Top*: specular point track overpasses of the Pascagoula River by CYGNSS in April 2019. *Bottom*: reflectivity track during each overpass. The river crossings are highlighted in red and the Associated GNSS-R Width of the river is given by the width of the least squares polynomial fit to the reflectivity [8].

5. SUMMARY

CYGNSS is able to resolve inland water bodies with significantly finer spatial resolution than its observations of most open ocean or land surfaces due to the coherent nature of scattering from smooth surfaces. This capability, combined with the frequent temporal sampling afforded by its constellation of 8 spacecraft, enables the measurement of rapidly changing water body extent. Examples of this are flood inundation caused by a hurricane landfall, seasonal flooding of a river delta caused by monsoon rains, and rivers overtopping their banks due to excessive stream flow. There are a wealth of potential uses for these capabilities, in both the hydrological sciences and applications such as disaster management. For example, resolving wetland extent under cloud cover and a vegetation canopy with CYGNSS can improve the tracking of methane emission [12].

REFERENCES

[1] Ruf, C., M. Unwin, J. Dickinson, R. Rose, D. Rose, M. Vincent and A. Lyons, "CYGNSS: Enabling the Future of Hurricane Prediction," IEEE Geosci. Remote Sens. Mag., 1(2), 52-67, doi: 10.1109/MGRS.2013.2260911, 2013.

[2] Unwin, M., P. Jales, P. Blunt, S. Duncan, M. Brummitt, C. Ruf, "The SGR-ReSI and its application for GNSS reflectometry on the NASA EV-2 CYGNSS mission," 2013 IEEE Aerospace Conference, Big Sky, MT, 2013, pp. 1-6, doi: 10.1109/AERO.2013.6497151.

[3] Bussy-Virat, C. D., C. S. Ruf, A. J. Ridley, "Relationship between temporal and spatial resolution for a constellation of GNSS-R satellites," IEEE J. Sel. Topics Appl. Earth Obs. Remote Sens., doi: 10.1109/JSTARS.2018.2833426, 2018.

[4] Gleason, S., C. Ruf, M. P. Clarizia, A. O'Brien, "Calibration and Unwrapping of the Normalized Scattering Cross Section for the Cyclone Global Navigation Satellite System (CYGNSS)," IEEE Trans. Geosci. Remote Sens., 54(5), 2495-2509, doi:10.1109/TGRS.2015.2502245, 2016.

[5] Clarizia, M. P., and C. S. Ruf, "Wind Speed Retrieval Algorithm for the Cyclone Global Navigation Satellite System (CYGNSS) Mission," IEEE Trans Geosci. Remote Sens., 54(8), doi:10.1109/TGRS.2016.2541343, Aug. 2016.

[6] Ruf, C. S., S. Asharaf, R. Balasubramaniam, S. Gleason, T. Lang, D. McKague, D. Twigg, D. Waliser, "In-Orbit Performance of the Constellation of CYGNSS Hurricane Satellites," Bull. Amer. Meteor. Soc., 2009-2023, doi: 10.1175/BAMS-D-18-0337.1, Oct. 2019.

[7] Loria, E., A. O'Brien, V. Zavorotny, B, Downs, C. Zuffada, "Analysis of scattering characteristics from inland bodies of water observed by CYGNSS," Remote Sens. Environ., doi: 10.1016/j.rse.2020.111825, 2020.

[8] Warnock, A., C. Ruf, "Response to Variations in River Flowrate by a Spaceborne GNSS-R River Width Estimator," Remote Sens., 11(20), 2450, doi: 10.3390/rs11202450, 2019.

[9] Zavorotny, V., A. Voronovich, "Scattering of GPS signals from the ocean with wind remote sensing applications," IEEE Trans. Geosci. Remote Sens. 38(2), 951–964, 2000.

[10] Camps, A., "Spatial Resolution in GNSS-R Under Coherent Scattering," Geosci. Remote Sens. Ltrs, doi: 10.1109/LGRS.2019.2916164, 2019.

[11] Gerlein-Safdi, C., C. S. Ruf, "A CYGNSS-Based Algorithm for the Detection of Inland Waterbodies," Geophys. Res. Ltrs., doi: 10.1029/2019GL085134, 2019.

[12] Gerlein-Safdi, C., A. Bloom, G. Plant, E. A. Kort, C. S, Ruf, "Improving representation of tropical wetland methane emissions with CYGNSS inundation maps, Earth and Space Science Open Archive, doi; 10.1002/essoar.10504845.1, 2020.